Asian Journal of Chemistry Vol. 22, No. 10 (2010), 8007-8016

Study on the Interaction of Amoxicillin and DNA by Spectroscopic and Voltammetric Studies

R. HAJIAN*, N. SHAMS and N. AZARINEZHAD
Young Researchers Club, Department of Chemistry, College of Science, Islamic Azad University Branch of Gachsaran, Gachsaran 75818-63876, Iran
Fax: (98)(742)3334750; Tel: (98)(742)3334751
E-mail: hajian@iaug.ac.ir

Spectrophotometric and voltammetric methods were used to probe the interaction of antimicrobial drug amoxicillin with calf thymus DNA (CT-DNA). Binding constants (K) and binding site sizes (s) were determined from the voltammetric data, *i.e*., shifts in potential and changes in limiting current with the addition of CT-DNA. Amoxicillin showed appreciable electrostatic binding to CT-DNA in solution with $K = 2.7 \times 10^4$ mol^{-1} L and s =0.42 bp. Methylene blue have been used as a probe for distinguish the mode of interaction between drug and CT-DNA. The voltammetric behaviour of amoxicillin has been investigated at a glassy carbon modified with multiwalled carbon nano tubes (MWCNTs) using cyclic voltammetry. The apparent transfer coefficients (α) and the number of electron transferred (n) of amoxicillin in the absence and presence of CT-DNA have determined using anodic Tafel plots of amoxicillin and amoxicillin-CT-DNA adduct on the surface of modified glassy carbone electrode. The slopes of the calibration curves for amoxicillin in the absence and presence of CT-DNA are significantly differing with each other that demonstrate a mode of interaction. Both UV-vis spectrophotometry and cyclic voltammetry studies confirmed the groove binding interaction between amoxicillin and CT-DNA.

Key Words: Amoxicillin, Methylene blue, Calf thymus DNA, Spectroscopy, Voltammetry, Groove binding.

INTRODUCTION

Deoxyribonucleic acid (DNA) plays a central role in life processes since it contains all of the genetic information required for cellular function. However, DNA molecules are prone to be damaged under various conditions, especially by interaction with some molecules and this damage may lead to various pathological changes in living organisms. There is growing interest in exploring the binding of small molecules with DNA for the rational design and construction of new and more efficient drugs targeted to DNA as well as in understanding how proteins recognize and bind to specific DNA sequences[1-3]. The specific interaction between a drug and DNA results in some changes in physical and chemical properties and has a potential importance for a better understanding of its therapeutic efficiency, which may also be used for conformational recognition to find new structures of

DNA[4-6]. Various techniques have been extensively employed to study the interaction of these molecules with DNA, such as spectroscopic methods[7-11], isothermal calorimetric titration[12], nuclear magnetic resonance[13], quartz crystal microgravimetry[14], *etc*. Since many small molecules exhibit redox activity, electrochemical method should provide a useful complement to the previously used methods for investigation[15-18]. Moreover, the electrochemical behaviours are valuable in elucidating some mechanisms of the drug action *in vivo*[19,20]. Although the binding modes of several molecules with large conjugated structures have been delineated and much less attention was paid to the binding of simple heterocyclic compounds.

Amoxicillin (AMX) (Fig. 1) ((2S,5R,6R)-6-[(R)-(–)-2-amino-2-(*p*-hydroxyphenyl) acetamido]-3,3-dimethyl-7-oxo-4-thia-1- azabicyclo [3.2.0] heptane-2-carboxylic acid trihydrate), is a semisynthetic antibiotic, an analog of ampicillin, with a broad spectrum of bactericidal activity against many gram-positive and gram-negative microorganisms. It has been extensively used in the treatment of infections of the lower respiratory tract, ear, nose and throat[21,22] but little is known about its interaction with DNA of cells.

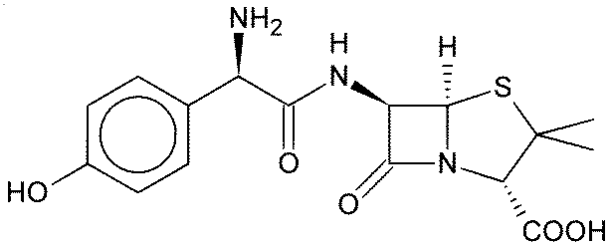

Fig. 1. Chemical structure of amoxicillin

In this report we explored the interaction of amoxicillin with calf thymus DNA (CT-DNA), using spectrophotometric and voltammetry techniques. The aim of this study is to find a relation between the antibacterial properties of drug and the mode of DNA binding. Because of the known interaction mechanism between methylene blue and DNA[23-28], it was used as a probe. This report offers an opportunity to understand how the structure of molecules affects their binding mode and binding affinity to DNA, which will help us to design new drugs, with biological and antitumour activity.

EXPERIMENTAL

Stock solution (1×10^{-3} mol L^{-1}) of amoxicillin was prepared by dissolving 0.0364 g of amoxicillin (three hydrates) with doubly distilled water in a 100 mL volumetric flask. A 1×10^{-3} mol L^{-1} methylene blue solution was prepared by dissolving 0.0374 g of methylene blue (Merck) in doubly distilled water and the solution was diluted in a 100 mL volumetric flask and kept in a refrigerator at 4 ºC. More dilute solutions were prepared by serial dilution.

Calf thymus DNA was used without further purification and bought from Fluka. Its concentration was determined spectrophotometrically using the molar absorptivity value, ε_{260} = 6600 mol^{-1} cm^{-1} [26]. For making a 1.76×10^{-4} mol L^{-1} DNA, 0.010 g of calf thymus DNA was dissolved in 0.010 mol L^{-1} phosphate buffer (pH = 7.4) and 0.05 mol L^{-1} sodium chloride solution in a 25 mL volumetric flask.

The multiwalled carbon nanotubes (MWCNT) were bought from Iran's Research Institute of Petroleum Industry and synthesized by chemical vapour deposition (CVD) with a diameter of 8-15 nm, a length of 50 μm and the purity of 95 %.

All diluted solutions were adjusted with the phosphate buffer (0.01 mol L^{-1}, pH 7.4) in the presence of 0.05 mol L^{-1} sodium chloride.

Voltammetric measurements were carried out using an EG and G instrument, Model 394. The GCE-MWCNT, a platinum electrode and a saturated Ag/AgCl reference electrode were employed as a working, auxiliary and reference electrodes, respectively.

UV-Vis absorption spectra were measured on an Agilent UV-vis spectrophotometer, Perkin-Elmer, with the use of 1 cm quartz cells.

Preparation of multiwalled carbon nanotubes suspension and modified glass calomel electrode (GCE): To eliminate metal oxide catalysts within the nanotubes, multiwalled carbon nanotubes were refluxed in the 2 mol L^{-1} HNO_3 for 15 h and then washed with double-distilled water and dried at room temperature. The purified MWCNTs were dispersed in acetonitrile (0.1 mg MWCNTs/10 mL) by using ultrasonic agitation to obtain a relative stable suspension. The glass calomel electrode was carefully polished with 0.05 mm alumina slurry on a polishing cloth and then washed ultrasonically in methanol and water, respectively. The cleaned GCE was coated by casting 300 mL of the black suspension of MWCNTs and dried in an oven at 60 °C. The microscopic area of the MWCNT-modified GCE was obtained by cyclo voltammetry using 1 mmol L^{-1} $K_3Fe(CN)_6$ as a probe at different scan rates. For a reversible process, the Randles-Sevcik formula has been used:

$$I_{pa} = 2.69 \times (AS\,mol^{-1}\,V^{-1/2}) n^{3/2} A C_0 D_R^{1/2} \nu^{1/2} \quad (1)$$

where I_{pa} (A) refers to the anodic peak current, n = electron transfer number, A (cm^2) = surface area of the electrode, D_R (cm^2 s^{-1}) is diffusion coefficient, C_0 (mol cm^{-3}) = concentration of $K_3[Fe(CN)_6]$ and ν (V s^{-1}) = scan rate. For 1 mmol L^{-1} $K_3[Fe(CN)_6]$ in the 0.1 mol L^{-1} KCl electrolyte: n = 1 and $D_R = 7.6 \times 10^{-6}$ cm^2 s^{-1}, then from the slope of the i_{pa} - $\nu^{1/2}$ relation, the microscopic areas can be calculated. On the bare GCE modified with MWCNT, the microscopic area was 0.074 cm^2.

RESULTS AND DISCUSSION

Spectrophotometric studies

Interaction of amoxicillin with CT-DNA: UV-Vis absorption spectra have been obtained by titration of 100 μmol L^{-1} AMX solution with increasing concentration of CT-DNA (Fig. 2). There were two absorption bands with maximum wavelengths

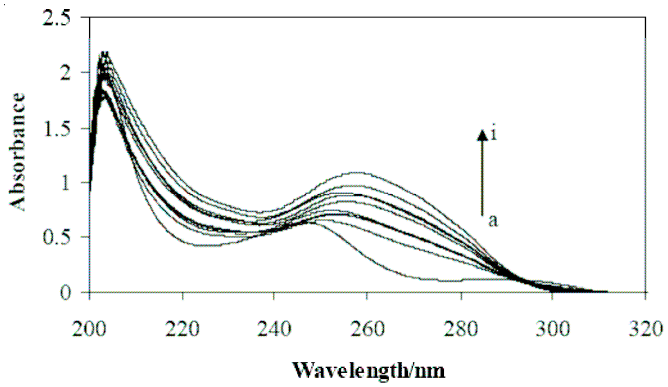

Fig. 2. Absorption spectra of AMX in the presence of CT-DNA at different concentrations. C_{DNA} = 0, 5, 10, 15, 20, 25, 30, 35 and 40 μmol L^{-1} for curves a-i and C_{AMX} = 50 μmol L^{-1} in phosphate buffer (0.01 mol L^{-1}, pH 7.4) plus NaCl (0.05 mol L^{-1})

at 204 nm and 260 nm in the absenence of CT-DNA. With increasing of CT-DNA concentration, the absorption bands increased continuously due to the highly overlapping spectra. In a similar way, the spectrum of CT-DNA in the absence of AMX was studied at different CT-DNA concentrations (Fig. 3). The significant difference at the slopes of two calibration curves in the absence and presence of AMX demonstrates that a small molecule such as AMX could affected on the structure of CT-DNA (Fig. 4).

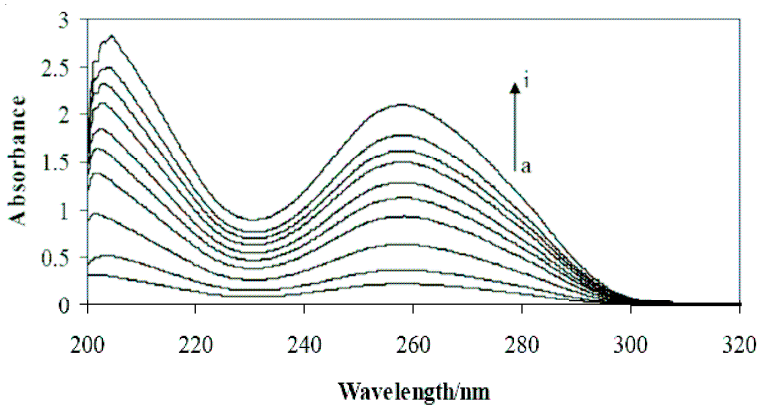

Fig. 3. Absorption spectra of CT-DNA in different concentrations: C_{DNA} = 24.6, 49.2, 73.8, 98.4, 123.0, 147.6, 172.2, 196.8, 221.4 and 246.0 μmol L^{-1} for curves a-j, in phosphate buffer (0.01 mol L^{-1}, pH 7.4) plus NaCl (0.05 mol L^{-1})

Furthermore the UV-vis absorption spectra have been obtained by titration of 20 μmol L^{-1} CT-DNA solutions with increasing concentration of AMX (Fig. 5). As can be seen in Fig. 6, the slopes of two calibration curves in the absence and presence of CT-DNA are significantly differ with each other due to the drug-DNA interaction.

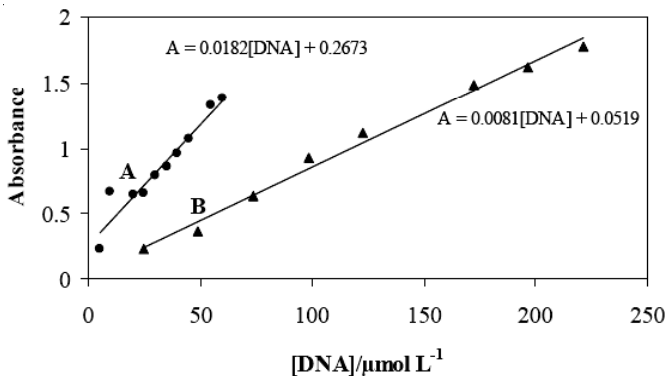

Fig. 4. Calibration curves of CT-DNA in the absence (A) and presence (B) of AMX at λ = 260 nm. Conditions: (A) C_{DNA}: 24.6, 49.2, 73.8, 98.4, 123.0, 172.2, 196.8 and 221.4 µmol L^{-1}; (B) C_{DNA}: 5.0, 10.0, 15.0, 20.0, 25.0, 30.0, 35.0, 40.0, 45.0, 55.0 and 60.0 µmol L^{-1}; C_{AMX}: 20 µmol L^{-1}

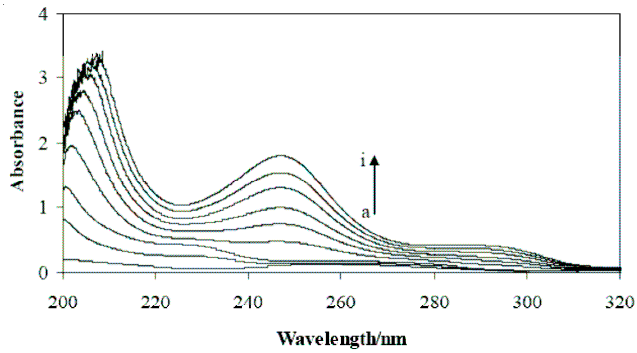

Fig. 5. Absorption spectra of CT-DNA in the present of AMX at different concentrations. C_{AMX} = 0, 20, 40, 60, 80, 100, 140, 160 and 180 µmol L^{-1} for curves a-i and C_{DNA} = 20 µmol L^{-1} in phosphate buffer (0.01 mol L^{-1}, pH 7.4) plus NaCl (0.05 mol L^{-1})

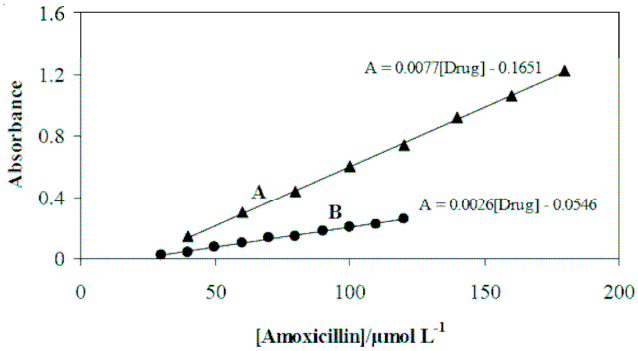

Fig. 6. Calibration curves of AMX in the absence (A) and presence (B) of CT-DNA at λ = 227 nm. Conditions: (A) C_{AMX}: 30, 40, 50, 60, 70, 80, 90, 100, 110 and 120 µmol L^{-1}; (B) C_{AMX}: 40, 60, 80, 100, 120, 140, 160 and 180 µmol L^{-1}; C_{DNA}: 40 µmol L^{-1}

In order to clarify the portion of AMX interacting with CT-DNA, the inclusion complex of methylene bule-CT-DNA has been used to further study the interaction site by a spectroscopic method.

Interaction of methylene blue with CT-DNA: Absorption spectra of methylene blue dye in the absence and presence of CT-DNA (pH 7.4) showed a maximum peak at 662 nm (Fig. 7). This peak gradually decreased with increasing the concentration of CT-DNA and red shift was usually associated with molecular intercalation into the base stack of the CT-DNA[10,29]. These two observed spectral effects were attributed to a strong interaction between the electronic state of the intercalating chromophore and the CT-DNA bases. The strength of this electronic interaction was expected to decrease as the cube of the distance between the chromophore and the CT-DNA bases[28]. The observed large hypochromism during the interaction of the methylene blue dye with the CT-DNA strongly suggests that the distance between the intercalated methylene blue dye and the CT-DNA bases be small. Thus, this is consistent with the rationalization that on intercalation of the methylene blue dye into the CT-DNA, the π-electrons of methylene blue combine with the π-electrons of CT-DNA and the empty π* orbital of methylene blue couples with the π orbital of the bases[28], which facilitates a decrease in the energy of the π-π* electron transition, causing a red shift. At the same time, the empty π* orbital is partially filled by electrons, reducing the π-π* transition probability, which contributes to the hypochromic effect discussed above.

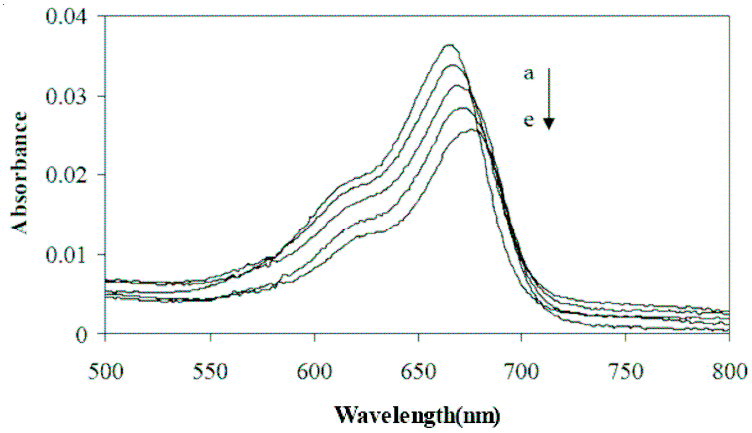

Fig. 7. Absorption spectra of methylene blue in the presence of CT-DNA at different concentrations: C_{DNA}= 0.0, 11.7, 23.4, 35.1 and 46.8 μmol L^{-1} for curves a-e and C_{MB} = 1.0 μmol L^{-1} in phosphate buffer (0.01 mol L^{-1}, pH 7.4) plus NaCl (0.05 mol L^{-1})

Competitive interaction of AMX with methylene blue-CT-DNA: The observed band of methylene blue-CT-DNA adduct at 668 nm have not changed significantly by increasing concentration of added AMX and no shift towards the blue or red end of the spectrum had observed. A new peak at wavelength < 300 nm increased progressively

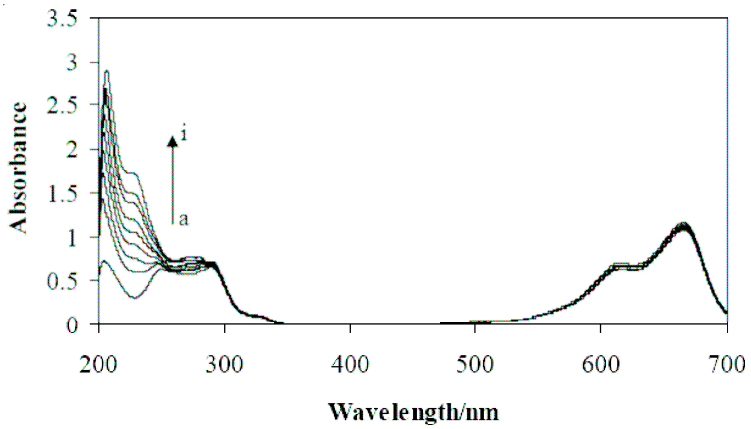

Fig. 8. Absorption spectra of the competitive reaction between AMX and methylene blue bonded to CT-DNA at C_{AMX} = 0.0, 24.0, 49.2, 73.8, 98.4, 123.0, 147.6, 172.2 and 196.8 μmol L^{-1} for curves a-i, C_{MB} = 100.0 μmol L^{-1} and C_{DNA} = 100 μmol L^{-1} in phosphate buffer (0.01 mol L^{-1}, pH 7.4) plus NaCl (0.05 mol L^{-1})

in intensity due to the added AMX (Fig. 8). The observed changes in intensity of the band with increasing amounts of AMX added to the MB-CT-DNA solution, suggested that AMX could not diffuses into the double helix of DNA adduct and exchanging with methylene blue.

Determination of viscosity: One indication of CT-DNA binding mode is the change in viscosity when a small molecule associates with CT-DNA. Intercalative binding increases the length of CT-DNA and the viscosity significantly, whereas groove binding typically has a smaller effect on viscosity[30]. Fig. 9 reveals that the viscosity of CT-DNA has not affected by the addition of AMX up to 3.2 times (AMX/DNA). It supports the groove binding for AMX with CT-DNA.

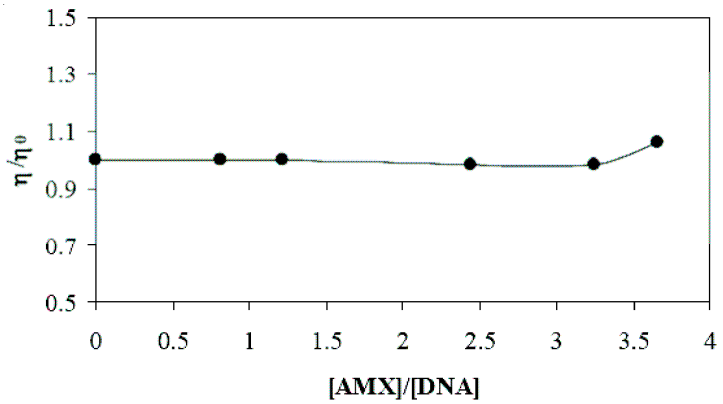

Fig. 9. Effect of AMX on the viscosity of CT-DNA solution. Amoxicillin was titrated into a 14.6 μmol L^{-1} DNA solution in concentration range of 0, 20, 30, 60, 80 and 90 μmol L^{-1} at 298 K

Electrochemical studies

Interaction of AMX with CT-DNA: The electrochemical behaviours of AMX in the absence and presence of CT-DNA at bare GCE-MWCNTs were studied by cyclic voltammetry. A single CV oxidation peak of AMX was observed at 0.76 V *versus* SCE in pH 7.4 phosphate buffer. The absence of any peaks in the reverse scan revealed the irreversible nature of the oxidation. The addition of CT-DNA into the AMX solution caused a considerable diminution in peak current as shown in Fig. 10. The binding of AMX to CT-DNA should lead to a significant decrease of AMX peak current due to the formation of AMX-CT-DNA adduct with very small diffusion coefficient[31,32]. This is obvious from the significant decrease in the slopes of linear I_p - $v^{1/2}$ plots in the absence and presence of CT-DNA with the equations of $I_p = 4.75 \times 10^{-4} (\pm 8.0 \times 10^{-6}) - 5.4 \times 10^{-5} (3.0 \times 10^{-6})$ and $I_p = 4.10 \times 10^{-4} (\pm 6.0 \times 10^{-5}) - 4.0 \times 10^{-5} (7.0 \times 10^{-6})$, respectively.

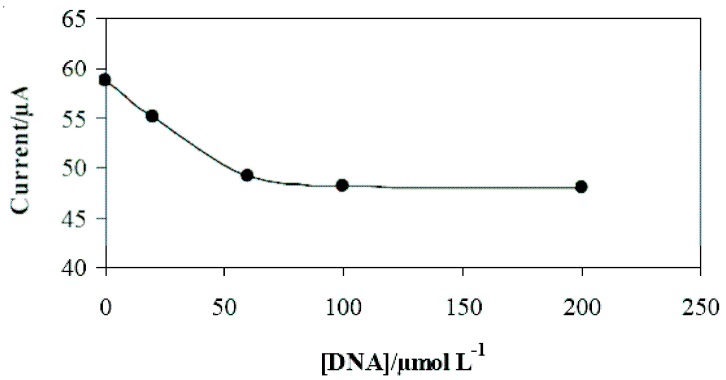

Fig. 10. Dependence of I_p of 10.0 μmol L^{-1} AMX on the added CT-DNA by cyclic voltammetry at the GC-MWCNTs. Scan rate = 13.3 mV/s

For the irreversible redox reaction of AMX, an αn_a value (α, the electron transfer coefficient; n_a, the number of electrons involved in the rate-determining step) can be evaluated as 0.94 and 0.96 for free AMX and AMX-CT-DNA adduct based on the slope of Tafel plots. From these values, a diffusion coefficient (D_f) of the free AMX was found to be 5.4×10^{-3} cm^2 s^{-1}, whereas $D_b = 1.4 \times 10^{-6}$ cm^2 s^{-1} was calculated for the bound AMX-CT-DNA.

For an irreversible reaction at 25 ºC, the peak current (I_p) of AMX can be calculated[33]:

$$I_p = B[(\alpha n_a)_f^{1/2} D_f^{1/2} C_f + (\alpha n_a)_b^{1/2} D_b^{1/2} C_b] \quad (2)$$

where $B = 2.99 \times 10^5$ $nAv^{1/2}$ [34], A = surface area of the working electrode, C_b and C_f represents the equilibrium concentration of AMX (bonded in AMX-DNA) and the concentration of free AMX and the total concentration of AMX, CT-DNA, is

$$C_t = C_f + C_b \quad (3)$$

Based on Carter *et al.*[35], the binding constant, K, can be expressed as the following form:

$$K = \frac{C_b}{C_f\left(\frac{[NP]}{2s} - C_b\right)} \quad (4)$$

where s = size of binding site in terms of bp and NP is DNA concentration. Making appropriate substitutions and eliminating C_b and C_f from eqn. 2, a new equation was obtained:

$$I_p = B\left\{(\alpha n_a)_f^{1/2} D_f^{1/2} C_t + [(\alpha n_a)_b^{1/2} D_b^{1/2} D_b^{1/2} - (\alpha n_a)_f^{1/2} D_f^{1/2}] \times \left[\frac{b - \left(b^2 - \frac{2K^2 C_t [NP]}{s}\right)^{1/2}}{2K}\right]\right\} \quad (5)$$

where $b = 1 + KC_t + K[NP]/2s$. Since I_p, C_t and [NP] are experimentally measurable and $(\alpha n_a)_f$, $(\alpha n_a)_b$, D_f and D_b have already been acquired as mentioned above, the binding constant (K) and binding site size (s) of the AMX-DNA can be obtained from a nonlinear regression analysis of the experimental data (I_p-[NP] plot) according to eqn. 5. For the binding curve (Fig. 10), a nonlinear fit analysis yielded $K = 2.7 \times 10^4$ mol^{-1} L and s = 0.42. Obviously, the interaction between AMX and the solution-phase CT-DNA was not as strong as some other aromatic compounds which could intercalate into DNA helix *via* large conjugated structures.

Conclusion

Studies on the binding of drugs with proteins were of great importance in pharmacy, pharmacology and biochemistry. Interaction between AMX and DNA was studied by UV-vis absorption spectra, cyclic voltammetry and viscometry. In solution, the drug AMX can bind to CT-DNA with a binding constant of $K = 2.7 \times 10^4$ mol^{-1} L and s = 0.42 bp, which were successively determined in this work by voltammetric method. The apparent transfer coefficients (α) and the number of electron transferred (n_a) of amoxicillin in the absence and presence of DNA have determined using anodic Tafel plots of amoxicillin and amoxicillin-DNA adduct on the surface of modified glassy carbon electrode. Both spectroscopy and electrochemistry techniques demonstrate a groove binding interaction between AMX and CT-DNA in solution.

ACKNOWLEDGEMENT

The authors gratefully acknowledged the financial support of this work by Islamic Azad University Branch of Gachsaran (IAUG).

REFERENCES

1. B. Lambert, J.B. Lepecq, W. Guschlbauer and W. Saenger, DNA-Ligand Interactions From Drugs to Proteins, Plenum, New York, p. 141 (1986).
2. M.P. Singh, T. Joseph, S. Kumar, Y. Bathini and J.W. Lown, *Chem. Res. Toxicol.*, **5**, 597 (1992).
3. D. Porschke, W. Guschlbauer and W. Saenger, DNA-Ligand Interactions, Specificity and Dynamics of Protein-Nucleic Acid Interactions, Plenum, New York, p. 85 (1986).

4. J.H. Griffin and P.B. Dervan, *J. Am. Chem. Soc*., **109**, 6840 (1987).
5. A.M. Pyle, J.P. Rehmann, R. Meshoyrer, C.V. Kumar, N.J. Turro and J.K. Barton, *J. Am. Chem. Soc*., **111**, 3051 (1989).
6. E. Palecek and M. Fojta, *Anal. Chem*., **73**, 75A (2001).
7. C.V. Kumar and E.H. Asuncion, *J. Am. Chem. Soc*., **115**, 8547 (1993).
8. G.C. Zhao, J.J. Zhu and H.Y. Chen, *Spectrochim. Acta A*, **55**, 1109 (1999).
9. M.R. Arkin, E.D.A. Stemp, C. Turro, N.J. Turro and J.K. Barton, *J. Am. Chem. Soc*., **118**, 2267 (1996).
10. A.A. Ensafi, R. Hajian and S. Ebrahimi, *J. Braz. Chem. Soc*., **20**, 266 (2009).
11. R. Hajian, N. Shams and A. Parvin, *Chin. J. Chem*., **27**, 1055 (2009).
12. R.A. Hutchins, J.M. Crenshaw, D.E. Graves and W.A. Denny, *Biochemistry*, **42**, 13754 (2003).
13. K. Sandstrom, S. Warmlander, M. Leijon and A. Graslunda, *Biochem. Biophys. Res. Commun*., **304**, 55 (2003).
14. M. Aslanoglu, A. Houlton and B.R. Horrocks, *Analyst*, **123**, 753 (1998).
15. M.T. Carter, M. Rodriguez and A.J. Bard, *J. Am. Chem. Soc*., **111**, 8901 (1989).
16. S.A. Ozkan, Y. Ozkan and Z. Senturk, *J. Pharm. Biomed. Anal*., **17**, 299 (1998).
17. S.F. Lu, K.B. Wu, X.P. Dang and S.S. Hu, *Talanta*, **63**, 653 (2004).
18. N. Erk, *Anal. Bioanal. Chem*., **378**, 1351 (2004).
19. S. Bollo, L.J. Nunez-Vergara and J.A. Squella, *J. Electroanal. Chem*., **562**, 9 (2004).
20. P.C. Mandal, *J. Electroanal. Chem*., **570**, 55 (2004).
21. T. Hazir, L.M. Fox, Y.B. Nisar, M.P. Fox, Y.P. Ashraf, W.B. MacLeod, A. Ramzan, S. Maqbool, T. Masood, W. Hussain, A. Murtaza, N. Khawar, P. Tariq, R. Asghar, J.L. Simon, D.M. Thea and S.A. Qazi, *Lancet*, **371**, 49 (2008).
22. P. Ball, *Int. J. Antimicrob. Ag*., **30**, 113 (2007).
23. R.W. Armstrong, T. Kurucsv and V.P. Strauss, *J. Am. Chem. Soc*., **92**, 3174 (1970).
24. A. Erdem, K. Kerman, B. Meric and M. Ozsoz, *Electroanalysis*, **13**, 219 (2001).
25. C. Ohuigin, D.J. McConnell, J.M. Kelly and W.J.M. Van der Putten, *Nucl. Acids Res*., **15**, 7411 (1987).
26. B.S. Fujimoto, J.B. Clendenning, J.J. Delrow, P.J. Heath and M. Schurr, *J. Phys. Chem*., **98**, 6633 (1994).
27. S.O. Kelly, J.K. Barton, N.M. Jackson and M.G. Hill, *Bioconjugate Chem*., **8**, 31 (1997).
28. C.Z. Huang, Y.F. Li and P. Feng, *Talanta*, **55**, 321 (2001).
29. E.C. Long and J.K. Barton, *Acc. Chem. Res*., **23**, 271 (1990).
30. D.T. Breslin, J.E. Coury, J.R. Anderson, L. McFail-Isom, Y.Z. Kan, L.D. Williams, L.A. Bottomley and G.B. Schuster, *J. Am. Chem. Soc*., **119**, 5043 (1997).
31. I.S. Shehatta and M.S. Ibrahim, *Can. J. Chem*., **79**, 1431 (2001).
32. M. Aslanoglu and G. Ayne, *Anal. Bioanal. Chem*., **380**, 658 (2004).
33. S.F. Wang, T.Z. Peng and C.F. Yang, *Biophys. Chem*., **104**, 239 (2003).
34. A.J. Bard and L.R. Faulkner, Electrochemical Methods: Fundamentals and Applications, Wiley, New York (1980).
35. M.T. Carter, M. Rodriguez and A.J. Bard, *J. Am. Chem. Soc*., **111**, 8901 (1989).

(*Received*: 19 March 2010; *Accepted*: 31 July 2010) AJC-8931